Archives of Toxicology (2018) 92:2163–2174
https://doi.org/10.1007/s00204-018-2223-y

NANOTOXICOLOGY

Revisiting the stress paradigm for silica nanoparticles: decoupling of the anti-oxidative defense, pro-inflammatory response and cytotoxicity

Susanne Fritsch-Decker[1] · Clarissa Marquardt[1] · Tobias Stoeger[2] · Silvia Diabaté[1] · Carsten Weiss[1]

Received: 4 December 2017 / Accepted: 17 May 2018 / Published online: 24 May 2018

Abstract

Engineered amorphous silica nanoparticles (nanosilica) are widely used in industry yet can induce adverse effects, which might be classified according to the oxidative stress model. However, the underlying mechanisms as well as the potential interactions of the three postulated different tiers of toxicity—i.e. oxidative-, pro-inflammatory- and cytotoxic-stress response—are poorly understood. As macrophages are primary targets of nanoparticles, we used several macrophage models, primarily murine RAW264.7 macrophages, and monitored pro-inflammatory and anti-oxidative reactions as well as cytotoxicity in response to nanosilica at max. 50 µg/mL. Special attention was given to the activation of mitogen-activated protein kinases (MAPKs) as potential regulators of the cellular stress response. Indeed, according to the oxidative stress model, also nanosilica elicits an, albeit modest, anti-oxidative response as well as pronounced pro-inflammatory reactions and cytotoxicity in macrophages. Interestingly however, these three tiers of toxicity seem to operate separately of each other for nanosilica. Specifically, impeding the anti-oxidative response by scavenging of reactive oxygen species does not prevent the pro-inflammatory and cytotoxic response. Furthermore, blocking the pro-inflammatory response by inhibition of MAPKs does not impair cell death. As hazard assessment has been guided by the prevailing assumption of a dose-dependent coupling of sequential tiers of toxicity, identification of critical physico-chemical parameters to assist the safe-by-design concept should be enabled by simply monitoring one of the toxicity read-outs. Our results indicate a more complex scenario in the case of nanosilica, which triggers independent pleiotropic effects possibly also related to different material properties and primary cellular targets.

Keywords Nanoparticle · Silica · Inflammation · MAPK · Oxidative stress model · Macrophage

Introduction

Engineered amorphous silica nanoparticles (SiO_2–NPs, nanosilica) are the most abundant nanomaterials and are used in surface coatings and varnishes, as fillers, e.g. in plastics and tires, as adsorbent and trickling agents but also as a food additive and serve as support material for pharmaceutical products such as (Fruijtier-Pölloth 2016; Murugadoss et al. 2017) tablets. Novel composite SiO_2–NPs are already used in dental fillings and are promising multifunctional biomedical tools, e.g. for bio-imaging and drug delivery to support diagnosis and therapy of various diseases (Nyström and Fadeel 2012; Ambrogio et al. 2011; Tang et al. 2012; Moret et al. 2015). However, biological and potential toxic effects of SiO_2–NPs are still insufficiently understood. Although SiO_2–NPs are generally considered to be non-toxic some adverse effects have been described in cell culture as well

Susanne Fritsch-Decker and Clarissa Marquardt contributed equally.

Electronic supplementary material The online version of this article (https://doi.org/10.1007/s00204-018-2223-y) contains supplementary material, which is available to authorized users.

✉ Silvia Diabaté
silvia.diabate@kit.edu

✉ Carsten Weiss
carsten.weiss@kit.edu

[1] Karlsruhe Institute of Technology, Campus North, Institute of Toxicology and Genetics, Hermann-von-Helmholtz-Platz 1, 76344 Eggenstein-Leopoldshafen, Germany

[2] Institute of Lung Biology and Disease, Helmholtz Zentrum München - German Research Center for Environmental Health, Ingolstädter Landstraße 1, 85764 Neuherberg, Germany

as in animal models (Fruijtier-Pölloth 2016; Murugadoss et al. 2017). Upon inhalation, the induction of inflammation in the deep lung seems to be the critical effect. With the recent increase in research activities on hazard identification of nanomaterials numerous studies with various cell lines demonstrated cytotoxic effects of SiO_2–NPs from different sources and synthesis routes (Fruijtier-Pölloth 2016; Murugadoss et al. 2017) as well as modest genotoxicity in vitro (Maser et al. 2015; Haase et al. 2017). However, the precise mechanisms of action of nanosilica induced toxicity are unknown. A shared mode of toxic action of nanoparticles independent on chemical identity was previously hypothesized to be based on a tiered approach whereby increasing particle concentrations trigger ROS production followed by an enhanced anti-oxidative response to finally boost inflammation culminating in cell death (Nel et al. 2006). However, whether the three tiers are functionally linked and are dependent on the same physico-chemical properties of NPs is not well understood. Specifically, in case of nanosilica the interplay of the anti-oxidative and pro-inflammatory response as well as cell death has not been explored. Knowledge on the mechanisms of toxicity provoked by nanosilica is still scarce. A central pathway regulating the cellular stress response is constituted by the mitogen activated protein kinase (MAPK) cascade (Herrlich et al. 2008; Gaestel et al. 2009).

Previously, increased production of reactive oxygen species (ROS) and activation of MAPKs have been implicated in the pro-inflammatory and cytotoxic action of nanosilica in different cell types (Morishige et al. 2012; Lee et al. 2011).

In the present study we analyzed the effects of nanosilica on macrophages, which are central mediators of innate immunity and are critically involved in many diseases linked to chronic inflammation such as silicosis. The anti-oxidative and pro-inflammatory response as well as cell death were analyzed by detailed gene expression studies, cytokine release and different cytotoxicity read-outs. The role of ROS and MAPK in these different adverse reactions was addressed by inhibition of selective MAPKs and a ROS scavenger. Finally, the interconnection between nanosilica-induced anti-oxidative response, inflammation and cell death was explored.

Methods

Materials

Dulbecco's Modified Eagle's Medium (DMEM), medium supplements and phosphate-buffered saline without calcium and magnesium (PBS) were obtained from Life Technologies (Frankfurt, Germany). Fetal bovine serum (FBS) was from Sigma-Aldrich (Taufkirchen, Germany). Chemicals for sodium dodecylsulfate polyacrylamide gel electrophoresis (SDS–PAGE) were from Carl Roth (Karlsruhe, Germany). Enhanced chemiluminescence (ECL) reagents and bovine serum albumin (BSA) were from GE Healthcare (Freiburg, Germany). Lipopolysaccharide (LPS, from *Pseudomonas aeruginosa*), *N*-acetyl-L-cysteine (NAC), Hoechst33342 (Hoechst), propidium iodide (PI), and standard laboratory chemicals were supplied by Sigma-Aldrich (Taufkirchen, Germany). The MAP kinase inhibitors PD98059 (2′-amino-3′-methoxyflavone), SB203580 [4-(4-fluorophenyl)-2-(4-methylsulfinylphenyl)-5-(4-pyridyl)1H-imidazole] and SP600125 (1,9-pyrazoloanthrone) were purchased from Merck (Darmstadt, Germany). Anti-MK2, anti-phospho p38 (Thr180/Tyr182), anti-phospho ERK1/2 (Th202/Tyr204), anti-phospho JNK1/2 (Thr183/Tyr185), anti-phospho MKK3/6 (Ser189/207), anti-phospho MEK1/2 (Ser217/221), anti-phospho MKK4 (Thr261), anti-phospho MKK7 (Ser271/Thr275), anti-phospho c-Jun (Ser63), and anti-phospho MK2 (Thr334) were obtained from Cell Signalling (Frankfurt a.M., Germany). Anti-LaminB (M-20), anti-PCNA (PC-10), anti-MKK3/6 (H-90), anti-MEK1/2 (12-B), anti-MKK7 (H-160), anti-ERK1 (K-23), anti-JNK2 (D2), anti-c-Jun (H-79), and anti-p38 (c-20) were from Santa Cruz (Heidelberg, Germany). Secondary horseradish peroxidase (HRP)-conjugated antibodies were from DAKO (Hamburg, Germany). IRDye®800 coupled secondary antibodies were obtained from Biozol (Hamburg, Germany). The primers listed in Table S1 were purchased from Metabion (Martinsried, Germany). Aerosil®200 (SiO_2–NPs) were kindly provided by Evonik (Frankfurt, Germany). Cadmium oxide (CdO) particles were purchased from Merck (Darmstadt, Germany).

Preparation of particle suspensions for cell treatment

The particles were directly suspended in cell culture medium without FBS at 1 mg/mL. The suspensions were probe sonified (Branson Sonifier, 250, Schwäbisch Gmünd, Germany) for 50 s (50 duty cycles, output 5) right before preparing dilutions and addition to cells. Particles were tested for endotoxin with the chromogenic endpoint Limulus Amebocyte Lysate (LAL) assay (Lonza, Basel, Switzerland). Particle suspensions of 1 mg/mL in deionized water were centrifuged at 20,800*g* for 10 min and the supernatants were tested according to the instructions of the manufacturer. The result for each particle type was below the lower limit of quantification of the test (0.1 EU/mL). It was therefore excluded that endotoxin contributed to the biological responses of the test cells.

Cell culture and particle treatment

The murine macrophage cell line RAW264.7 was obtained from American Type Culture Collection (ATCC, Rockville, MD), and maintained in Dulbecco's Modified Eagle's Medium (DMEM) supplemented with 10% (v/v) FBS, 100 U/mL penicillin, and 100 mg/mL streptomycin (Life Technologies, Frankfurt, Germany). Human peripheral blood mononuclear cells (PBMC) were isolated from buffy coats derived from healthy donors (Städtisches Klinikum, Karlsruhe) by Ficoll density gradient centrifugation (Ficoll-Paque™ Premium, GE Healthcare, Freiburg). After washing the PBMC with phosphate-buffered saline (PBS, containing 0.5% BSA and 2 mM EDTA), the isolated cells were resuspended in RPMI 1640 medium supplemented with 10% FBS (v/v), 100 U/mL penicillin, 100 µg/mL streptomycin, 2 mM glutamine and cultivated in 5% CO_2 at 37 °C for 30 min. The non-adherent cells were washed out with warmed PBS and the adherent monocytes/macrophages were incubated in fresh medium at 37 °C in a humidified atmosphere containing 5% CO_2. After 24 h the monocytes/macrophages were detached from the surface using accutase and seeded into well plates at 1.5×10^5 cells/cm^2. To differentiate the monocytes to macrophages (monocyte derived macrophages, MDM), cells were cultivated in medium containing 2 ng/mL GM-CSF (granulocyte–macrophage colony-stimulating factor, Genscript, Piscataway, USA) for 14 days. After the first 7 days the medium was removed, centrifuged and the supernatant (conditioned medium) was supplemented with double concentrated GM-CSF. 50% of the conditioned medium was added to 50% of fresh medium and the cells were cultured for additional 7 days. The human monocytic cell line (THP-1) was purchased from DSMZ (Braunschweig, Germany) and maintained in RPMI1640 medium supplemented with 10% FBS (v/v), 100 U/mL penicillin, 100 µg/mL streptomycin at 37 °C with 5% CO_2. For experiments the monocytic THP-1 cells were differentiated with 100 nM PMA (phorbol myristate acetate). After 3 days the medium was removed and the adherent cells were cultured in fresh medium without PMA for additional 5 days.

Cells were seeded in appropriate cell culture dishes (either 6-, 24- or 96-well plates, see below) and particle treatment of cells was performed as described previously (Panas et al. 2013). On the day of exposure the cell culture medium was removed and replaced with half the volume of the required test medium (without serum; −/+ inhibitor) and incubated for 30 min. Subsequently, the second half of the final volume with or without particles (−/+ inhibitor) was added. Directly before treatment particle dilutions were vortexed to avoid sedimentation of particles and then added to the cells, which were exposed for the indicated time points. Solvent controls contained 0.1% dimethyl sulfoxide (DMSO) or 0.1% PBS. Final inhibitor concentrations were 5 mM NAC, 10 µM PD98059, 10 µM SB203580 and 10 µM SP600125.

Western blot analysis

For protein analysis cells were seeded into well plates ($1.5–2 \times 10^5$ cells/cm^2) and treated with particles in culture medium as described above. After exposure whole cell extracts were prepared and lysates were analyzed as described previously (Fritsch-Decker et al. 2011).

Enzyme-linked immunosorbent assay (ELISA)

Secretion of TNF-α, IL-6 and IL-1β was analyzed using specific OptEIA ELISA kits according to the manufacturer's instructions (BD Biosciences, Heidelberg, Germany).

Microscopy-based determination of cell counts, apoptosis and necrosis

For microscopic assays 2.5×10^4 cells/well were seeded in 96-well plates and exposed to particles in 100 µl culture medium as described above. Directly after exposure cells were incubated with 0.3 µg/mL Hoechst 33342 and 0.5 µg/mL PI for 30 min at 37 °C and 5% CO_2. Subsequently, four images per well were acquired using the automated fluorescence microscope IX81 (Olympus, Germany) with a 10-fold objective. Automated image analysis was carried out using the Olympus Scan® analysis software and data were analyzed and presented as described previously (Donauer et al. 2012; Hansjosten et al. 2018).

LDH assay

After treatment of cells with NPs the plates were centrifuged at 300×*g* for 5 min and the supernatants were analysed as described previously (Dilger et al. 2016). The relative amount of released lactate dehydrogenase (LDH) was normalized to the total amount of LDH of control cells which were completely lysed with 1% Triton X-100.

mRNA extraction and real-time PCR analysis

RAW264.7 cells (2×10^6) were seeded into each cavity of 6-well plates and treated with particles suspended in 3 mL culture medium on the next day. The total mRNA was extracted by disrupting cells using peqGold RNApure reagent (Peqlab, Erlangen, Germany) according to the manufacturer's instructions. The extracted mRNA was processed for real-time PCR analysis as described previously (Schreck et al. 2009). Glyceraldehyde 3-phosphate dehydrogenase (GAPDH) was employed as a reference housekeeping gene. The cDNA was used for detecting the expression of heme

oxygenase-1 (Hmox1), NADPH quinone oxidoreductase-1 (Nqo1), gamma-glutamylcysteine synthetase catalytic subunit (Gclc), inducible nitric oxide synthase (Nos2), cyclooxygenase-2 (Ptgs2), c-FOS (Fos) and the cytokines Cxcl2, interleukin-6 (Il6), interleukin-1β (Il1b), monocyte chemoattractant protein-1 (Ccl2), tumor necrosis factor-alpha (Tnf) and ribosomal protein, large, P0 (Rplp0) using the primer pairs listed in Table S1. The PCR amplification and real-time fluorescence quantification were performed in technical duplicates as previously described (Schreck et al. 2009) by using the ABI Prism 7000 (Applied Biosystems, Carlsbad, USA).

Statistical analysis

The results are expressed as means + standard deviation (SD) of several independent experiments as indicated in the legends and graphs, respectively. Normal distribution of data was confirmed by the Anderson–Darling test. The significance of difference between two mean values was assessed by Student's *t* test. A p value < 0.05 was considered to be statistically significant.

Results

Particle characterization

Nominal particle size and specific surface area of the SiO_2–NPs (Aerosil®200) were provided by the manufacturer as 12 nm and 200 ± 25 m^2/g, respectively. Previously we used transmission electron microscopy to study the size distribution, morphology and aggregation/agglomeration of the NP sample. NPs were nearly spherical and formed larger aggregates possibly due to sintering (Panas et al. 2013). Dynamic light scattering measurements (Table S2) showed that the size of SiO_2–NPs in the freshly prepared suspensions was similar in H_2O or cell culture medium (200–250 nm). Also, at 24 h no signs of further agglomeration were detected.

Next, we analyzed activation of the three different tiers of toxicity, i.e. the anti-oxidant and pro-inflammatory response as well as cytotoxicity, by nanosilica.

Nanosilica moderately activates an anti-oxidant response dependent on ROS

In contrast to the positive control cadmium oxide, nanosilica triggered only a modest anti-oxidative response at the gene expression and protein level (Fig. 1a–c) in line with our previous studies documenting the absence of a broad enhancement of intracellular ROS levels as detected by H_2DCF oxidation in RAW264.7 macrophages (Panas et al. 2013).

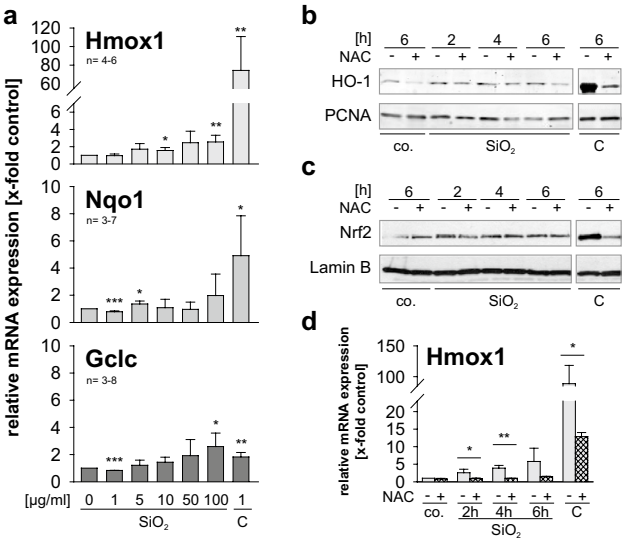

Fig. 1 Silica NPs induce a moderate anti-oxidative response dependent on ROS formation. **a** RAW264.7 macrophages were exposed to 1, 5, 10, 50 and 100 µg/mL SiO_2-NPs or to 1 µg/mL CdO (C) for 6 h and control cells to medium alone. mRNA levels of the anti-oxidative genes Hmox1 (HO-1), Nqo1 (NADPH quinone oxidoreductase-1), and Gclc (gamma-glutamylcysteine synthetase catalytic subunit) were analyzed by qRT-PCR and quantified relative to the untreated control. Results are given as means + SD from independent experiments (*$p < 0.05$; **$p < 0.01$ in comparison to the controls). RAW264.7 macrophages were pre-treated or not with 5 mM NAC and then exposed to 50 µg/mL SiO_2 NPs for 2, 4 and 6 h (**b**–**d**). Positive controls were exposed to 1 µg/mL CdO (C) and negative control cells to medium alone for 6 h. HO-1 (**b**) and Nrf2 protein (**c**) were analyzed in whole cell lysates by Western Blot. PCNA and Lamin B served as loading controls. The blots are representative for two independent experiments. **d** Expression of the Hmox1 gene was analyzed by qRT-PCR and quantified relative to the untreated control. Results are given as means + SD from three independent experiments (*$p < 0.05$; **$p < 0.01$ in comparison to the untreated controls)

Nevertheless, the ROS scavenger *N*-acetylcysteine (NAC) completely abolished induction of heme oxygenase-1 (HO-1) mRNA levels (Fig. 1d) consistent with previous studies in human breast cancer cells documenting localized oxidative stress in response to SiO_2–NPs indicated by mitochondrial generation of ROS and lipid peroxidation (Shi et al. 2012). In conclusion, SiO_2–NPs initiate a mild anti-oxidative response dependent on ROS.

Activation of the pro-inflammatory response by nanosilica

To address induction of the pro-inflammatory response by SiO_2-NPs we investigated changes in gene expression of selected marker genes. Whereas the mRNA levels of the pro-inflammatory genes encoding tumor necrosis factor-alpha (Tnf), cyclooxygenase-2 (Ptgs2), monocyte chemoattractant protein-1 (Ccl2) and chemokine ligand-2 (Cxcl2, also

known as MIP-2) were up-regulated after exposure to particles (Fig. 2a, S1a) inducible nitric oxide synthase (Nos2), interleukin-6 (Il6) and interleukin-1-beta (Il1b) were less prominently induced (Fig. S1a, b).

According to the temporal changes in gene expression, we categorized the various genes as early or delayed responders (Table S3). The early response genes, especially Tnf, might be responsible for induction of the delayed target genes such as Il-6 as published previously by others (Gaestel et al. 2009; Driscoll 2000).

As the regulation of cytokine expression is not exclusively controlled at the mRNA level but also involves multiple post-translational steps we also studied the final release of TNF-α, IL-6 and IL-1β. Whereas the amounts and release of TNF-α were increased after exposure to SiO_2-NPs (Fig. 2b, c) no strong release of IL-6 or IL-1β (data not shown) in the supernatants could be detected.

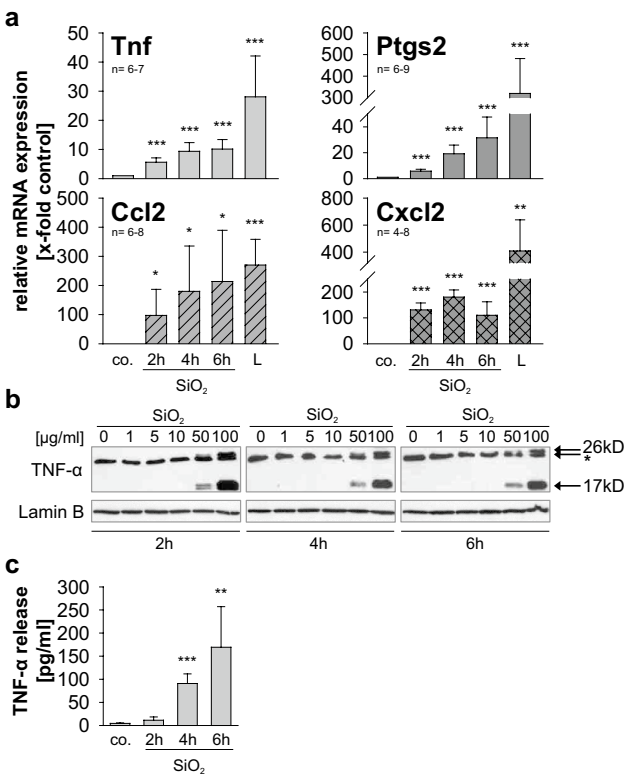

Fig. 2 SiO_2-NPs induce pro-inflammatory gene expression and increase protein levels and secretion of TNF-α. **a** RAW264.7 macrophages were exposed to 50 µg/mL SiO_2-NPs and to 1 µg/mL LPS (L) for 2, 4, and 6 h and control cells to medium alone. mRNA levels of the pro-inflammatory genes Tnf (TNF-α), Ptgs2 (COX-2), Cxcl2 (MIP-2) and Ccl2 (MCP-1) were analyzed by qRT-PCR and quantified relative to the untreated control. Results are given as means + SD from independent experiments (*$p < 0.05$; **$p < 0.01$; ***$p < 0.001$ in comparison to the untreated controls). **b** Cells were exposed to SiO_2-NPs and control cells to medium alone. Intracellular TNF-α was detected in whole cell lysates by Western blot using a specific antibody (26 kD unprocessed TNF-α, * unspecific, 17 kD cleaved TNF-α). Lamin B was used as a loading control. The blots are representative for three independent experiments. In **c** cells were exposed to 50 µg/mL SiO_2-NPs for 2, 4, and 6 h. The amount of TNF-α in the supernatant medium was quantified by ELISA. Results are given as means + SD from four independent experiments (**$p < 0.01$; ***$p < 0.001$ in comparison to the untreated controls)

Nanosilica provokes cell death

After 4 and more pronounced after 6 h increased leakage of the LDH could be detected (Fig. 3a). As LDH release

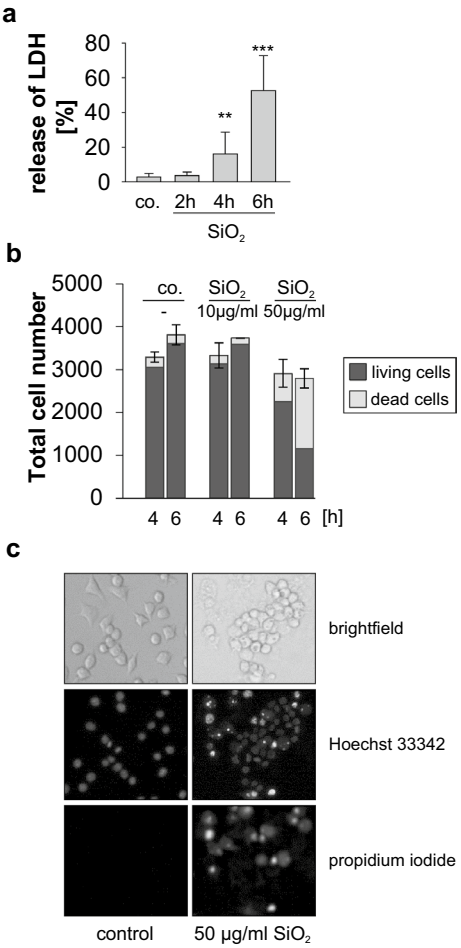

Fig. 3 SiO_2-NP induce cell death in dependence of dose and time. RAW264.7 macrophages were either exposed to 50 µg/mL SiO_2-NPs for 2, 4 and 6 h (**a**) or to 10 and 50 µg/mL SiO_2-NP for 4 and 6 h (**b**). Control cells received medium alone. **a** Membrane integrity was measured by LDH release into the culture medium. Results are given as means + SD from five independent experiments (**$p < 0.01$; ***$p < 0.001$ in comparison to the untreated controls). **b** Cell viability and cell death were assessed by automated, high-throughput microscopy as described under methods. Total cell number is depicted and divided into living and dead cells. Depicted are mean values ± SD of a representative experiment carried out with three up to four replicates. **c** Shown are representative images of macrophages exposed to SiO_2–NP for 6 h acquired in different channels (brightfield, Hoechst, propidium iodide)

is observed in necrotic but also late apoptotic cells we used microscopy to further analyze the mode of cell death induced by nanosilica. High (50 µg/mL) but not low concentrations (10 µg/mL) of SiO_2-NPs reduced cell counts and triggered cell death dependent on time (Fig. 3b). In line with the LDH assay, nanosilica promoted cell death is characterized by a simultaneous increase in chromatin condensation and membrane permeability reminiscent of late apoptosis (Fig. 3c).

The pro-inflammatory response and cytotoxicity induced by nanosilica is independent of ROS

Having established that all three tiers of toxicity are apparently simultaneously affected by nanosilica, we next explored the potential interdependencies of the different responses. As ROS are involved in the mild anti-oxidative response (Fig. 1) we addressed the role of ROS in nanosilica triggered pro-inflammatory responses and cytotoxicity. Co-incubation of cells with SiO_2–NPs and the anti-oxidant NAC did not abolish up-regulation of pro-inflammatory genes (Fig. 4 and S2) nor was cytotoxicity reduced as previously published (Marquardt et al. 2017). Hence, ROS seem to be important for the anti-oxidative response, i.e. regulation of heme oxygenase-1 expression but not for the other two tiers, i.e. the pro-inflammatory and cytotoxic response. Therefore, in the following, the impact of the MAPK cascade on the latter two responses was investigated.

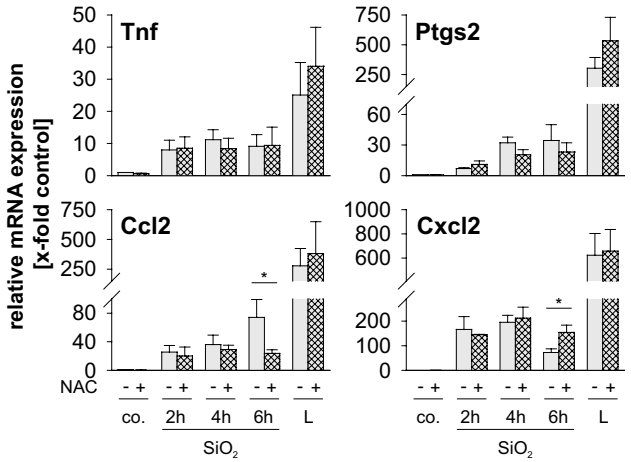

Fig. 4 The anti-oxidant NAC has no major impact on SiO_2–NP-induced expression of selected pro-inflammatory genes. RAW264.7 macrophages were pre-treated or not with 5 mM NAC and then exposed either to 50 µg/mL SiO_2-NPs for 2, 4 and 6 h. Positive controls to monitor gene activation were exposed to 1 µg/mL LPS (L) and negative control cells to medium alone for 6 h. mRNA levels were analyzed and results are presented as described in Fig. 2. Results are given as means + SD from three independent experiments (*$p < 0.05$ in comparison to the samples not treated with the antioxidant)

Role of the different MAPKs in pro-inflammatory gene expression induced by nanosilica

Exposure of cells to increasing concentrations of SiO_2–NPs induced the activation of all three mitogen activated protein kinases (MAPKs) ERK1/2, p38 and JNK1/2 (Fig. 5a). Phosphorylation of MAPKs was rapidly up-regulated and even stronger than after exposure to bacterial lipopolysaccharides (LPS), a known inducer of the MAPK pathway. In addition, we used particulate cadmium oxide as a reference, which also triggered MAPK phosphorylation to a similar extent albeit at much lower concentration. MAPK activation by SiO_2–NPs was accompanied by increased phosphorylation of the upstream MAP2 kinases (mitogen-activated protein kinase kinases) MKK1/2, MKK3/6 and MKK4 as well as enhanced activation of the relevant MAPK targets MK2 (mitogen-activated protein kinase (MAPK)-activated protein kinase-2) and c-Jun (Fig. S3).

In order to explore the relevance of the individual MAPKs p38, JNK1/2 and ERK1/2 for the pro-inflammatory response after nanosilica exposure we used selective inhibitors of the different kinases. The efficiency of the various MAPK inhibitors was validated by reduced phosphorylation of the kinase itself (ERK1/2) or its downstream substrates (c-Jun in case of JNK1/2 and MK2 in case of p38) after treatment with nanosilica (Fig. S4). Inhibition of p38 did not reduce induction of mRNAs transcribed from the Tnf-, Ptgs2-, Ccl2- and Cxcl2-genes (Fig. 5b). Only the modest increase of Il1b and Il6 transcripts seemed to be dependent on p38 activity whereas all the other genes remained more or less unaffected (Fig S5). Interference with JNK1/2 suppressed the elevation of the mRNA of Tnf at all and Cxcl2 at late time points (Fig. 5b). Of note, blocking JNK activity by the respective inhibitor increases p38 activation and vice versa inhibition of p38 enhances JNK phosphorylation (Fig. S4). As p38 promotes Il1b and JNK Tnf expression, even further enhanced activation of p38 or JNK in the presence of the respective inhibitor and nanosilica might explain the enhanced mRNA levels of the two genes (Fig. 5b and S5). This negative feedback loop between JNK and p38 has been observed previously (Wagner and Nebreda 2009). The strongest influence on nanosilica induced gene expression was observed for the inhibitor of the ERK1/2 pathway. Up-regulation of mRNAs expressed from the Ptgs2-, Ccl2- and Cxcl2- (Fig. 5b) and Il1b- genes (Fig. S5) was diminished. In summary, the MAPK JNK contributes primarily to the induction of Tnf, whereas ERK mediates regulation of Ptgs2, Ccl2 and Cxcl2 by nanosilica. Thus, in contrast to p38 the MAPK family members JNK and ERK seem to selectively contribute to pro-inflammatory gene expression in response to nanosilica. Noteworthy,

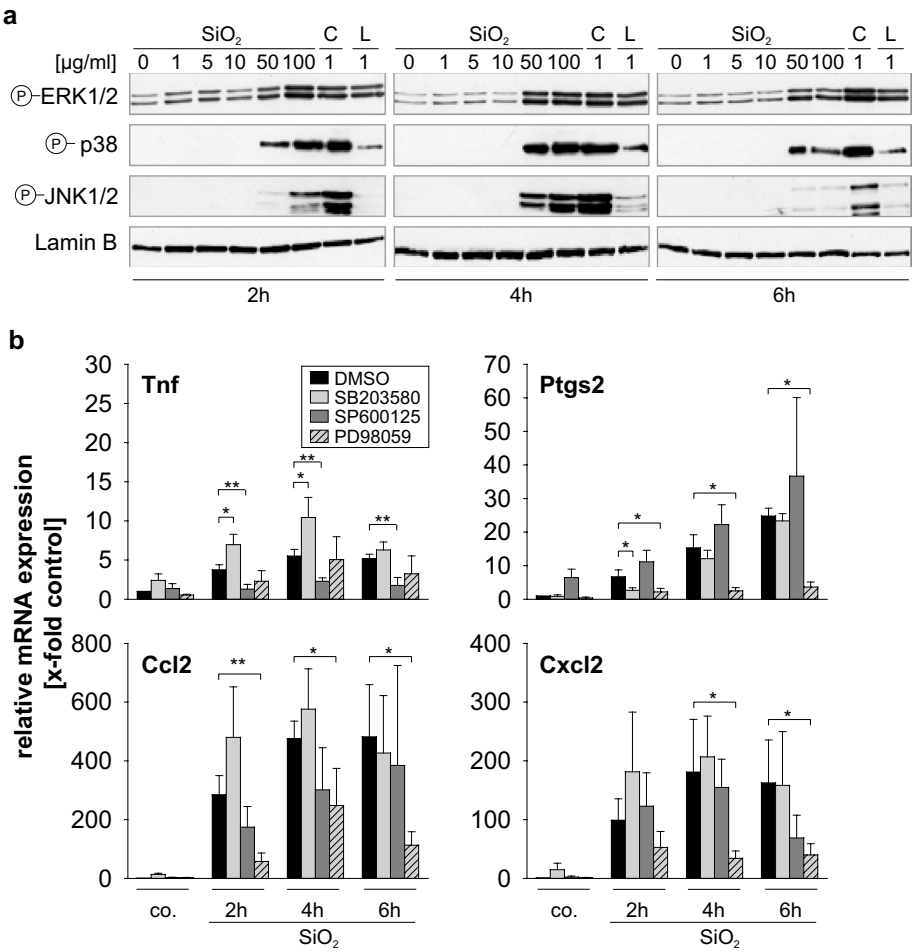

Fig. 5 SiO_2-NPs induce activation of MAPKs and inhibition of the MAPKs JNK1/2 and ERK1/2, but not p38, decreases pro-inflammatory gene expression initiated by SiO_2-NP. **a** RAW264.7 macrophages were exposed to the indicated concentrations of SiO_2-NPs, CdO (C) and LPS (L) for 2, 4 and 6 h and control cells to medium alone. Activation of MAP kinases was detected in whole cell lysates by Western blot using phospho-specific antibodies. Lamin B was used as a loading control. The blots are representative for three independent experiments. **b** RAW264.7 cells were pre-treated or not with 10 µM MAPK inhibitors SB203580 (p38 MAPK), SP600125 (JNK), PD98059 (ERK) or 0.1% DMSO for 30 min and then exposed to 50 µg/mL for 2, 4, and 6 h and control cells to medium alone. Cells were analyzed and results are presented as described in Fig. 2. Results are given as means + SD from 3 to 4 independent experiments (*$p < 0.05$; **$p < 0.01$; ***$p < 0.001$ in comparison to the samples not treated with inhibitor)

none of the MAPK inhibitors blocked induction of iNOS by LPS or nanosilica, presumably because iNOS is specifically regulated by the transcription factor NF-kappa B (Robinson et al. 2011).

As nanosilica exposure induced secretion of TNF-α we also tested the involvement of all three MAPKs by using the different inhibitors. As expected, inhibition of JNK1/2 prevented up-regulation of the TNF-α protein and its secretion (Fig. 6a, b). In addition, although inhibition of the ERK1/2 kinases did not interfere with the induction of TNF-α at the mRNA level (Fig. 5b) it clearly abrogated the increase of the TNF-α protein and its secretion in response to nanosilica (Fig. 6a, b). This finding is not too surprising as indeed ERK1 and 2 are involved in the complex control of TNF-α translation and release (Gaestel et al. 2009) and further highlight the importance to study all different levels of the multilayered process of cytokine secretion after exposure to nanosilica.

As the ROS scavenger NAC suppressed the anti-oxidant but not the pro-inflammatory response (Figs. 1, 4a), this suggested no major role of ROS for pro-inflammatory gene expression which, however, is controlled by MAPKs. In line with this hypothesis, co-treatment with NAC also did not abrogate MAPK activation by nanosilica (Fig. S6).

MAPK activation does not promote cell death induced by nanosilica

The concentrations of nanosilica required to induce MAPK activation (Fig. 5a) and pro-inflammatory responses (Fig.

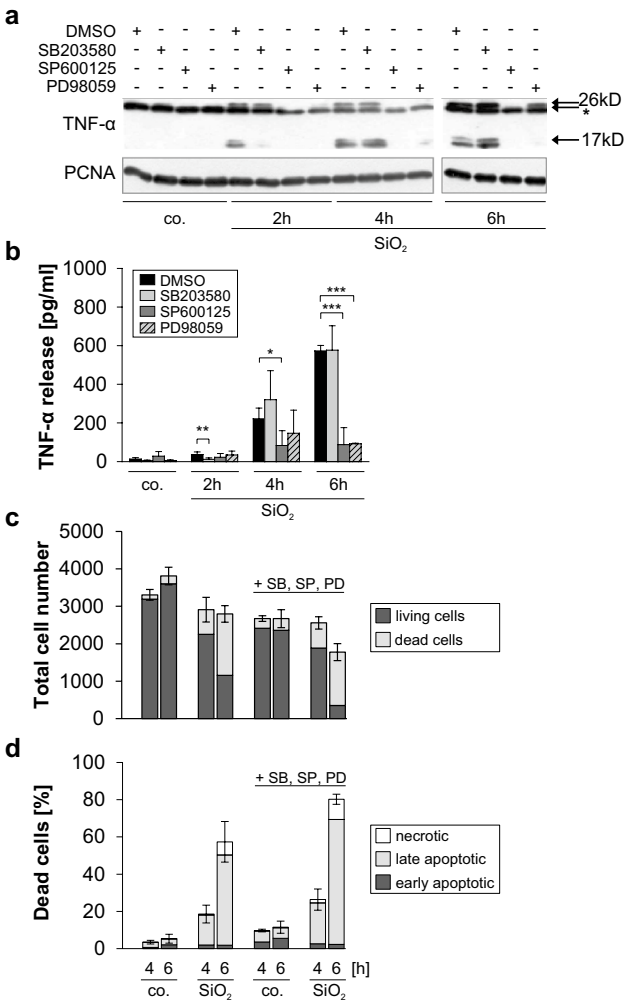

Fig. 6 Inhibition of the MAPKs JNK1/2 and ERK1/2 suppresses increased levels and release of TNF-α, but does not prevent cell death induced by SiO_2-NP. **a, b** RAW264.7 macrophages were pre-treated or not with 10 µM of the MAPK inhibitors SB203580 (p38 MAPK), SP600125 (JNK), PD98059 (ERK) or 0.1% DMSO for 30 min and then exposed to 50 µg/mL SiO_2-NPs for 2, 4, and 6 h and control cells to medium alone. **a** Intracellular TNF-α was detected in whole cell lysates by Western Blot using a specific antibody (26 kD unprocessed TNF-α, * unspecific, 17 kD cleaved TNF-α). PCNA (proliferating cell nuclear antigen) was used as a loading control. The blots are representative for three independent experiments. In **b** the supernatant medium was tested for TNF-α release by ELISA. Results are given as means + SD from three up to five independent experiments (*$p < 0.05$; **$p < 0.01$; ***$p < 0.001$ in comparison to the samples not treated with inhibitor). **c, d** Cell viability and cell death were assessed by microscopy as described under methods. RAW264.7 cells were pre-treated or not with a mixture of the MAPK inhibitors SB203580, SP600125 and PD98059 (each at 10 µM) or medium with DMSO solvent control for 30 min and then exposed to 50 µg/mL SiO_2–NPs for 4 and 6 h. **c** Cell death was analyzed as described above. **d** Percentage of dead cells relative to the total cell number divided into early apoptotic, late apoptotic and necrotic cells. Depicted are mean values ± SD of a representative experiment carried out with four replicates

S2) were also cytotoxic (Fig. 3). To address whether cytotoxicity was a consequence of excessive MAPK activation by nanosilica as suggested previously (Lee et al. 2011) we first studied the kinetics of both processes. Indeed, MAPK activation precedes the onset of membrane rupture, as it is already visible after 2 h and maximal after 4 h (Fig. S7). However, individual (data not shown) or combined inhibition of all three MAPK families does not prevent cell death induced by nanosilica (Fig. 6c, d). Hence, in macrophages MAPK activation and pro-inflammatory responses are separate events initiated by exposure to nanosilica and are not responsible for subsequent cell death.

MAPK signaling is also induced at non-toxic concentrations of nanosilica and in multiple cellular models

The interconnection between MAPKs and cell death is complex as MAPKs not only regulate cell death but vice versa are stimulated by dying cells (Zitvogel et al. 2010). In order to address whether silica nanoparticles can induce MAPK activation in the absence of cell death we performed more detailed dose response experiments to define sub-toxic concentrations. We realized that compared to late passages (cultured for more than 3 months) early passages (cultured for 2–6 weeks) of RAW264.7 macrophages were less sensitive to nanosilica provoked cytotoxicity (ca. 30 vs. 50% LDH release at 6 h, compare Fig. 7a to Fig. 3a). More important, doses which did not trigger LDH release (15 and 20 µg/mL) at any time point (2, 4 and 6 h) clearly induced MAPK phosphorylation. Furthermore, we also validated the critical role of the MAPKs ERK and JNK, but not p38, in the up-regulation of TNF-alpha at non-toxic concentrations (Fig. S8).

That MAPK activation by nanosilica in the absence of cytotoxicity is also observed in other cellular models from different species is shown in the human monocyte/macrophage cell line THP-1 and human macrophages derived from peripheral blood monocytes (Fig. 7b, c). Again a clear dose response is detected whereby low non-toxic concentrations induce MAPK phosphorylation and only at the highest concentrations additional membrane rupture occurs. In essence, activation of MAPKs and the pro-inflammatory response by nanosilica also occurs at lower non-toxic concentrations of nanosilica, i.e. in absence of cell death. At higher concentrations cytotoxicity ensues and this dose-dependent response is highly conserved in various types of murine and human macrophages.

In summary, for nanosilica we verified and refined the hierarchical stress model. Silica NPs trigger a weak antioxidative and a clear pro-inflammatory response dependent on ROS and MAPK signalling, respectively, whereas at high concentrations cell death ensues. The different tiers of toxicity act independent of each other and different

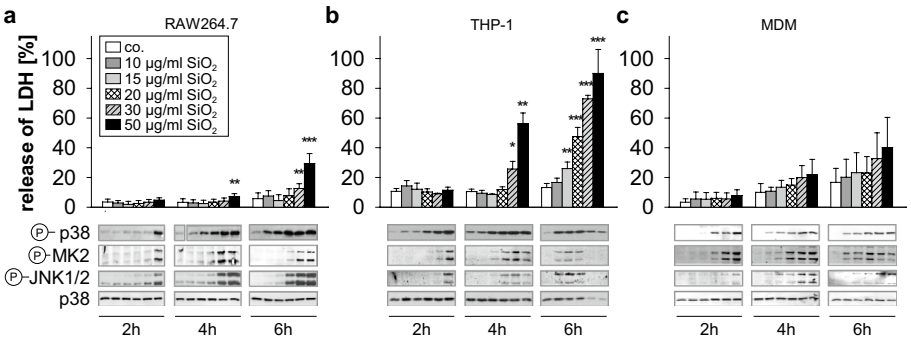

Fig. 7 Non-cytotoxic doses of silica NPs induce MAPK phosphorylation in transformed but also primary macrophages. Murine RAW264.7 (**a**), human THP-1 (**b**) and human monocyte-derived primary macrophages (MDM) (**c**) were treated with 10, 15, 20, 30 and 50 µg/mL silica NPs for 2, 4 and 6 h. LDH was analyzed in the supernatants. Results are given as means + SD from three independent experiments. Phosphorylation of p38, MK2 and JNK1/2 MAPKs was detected in whole cell lysates by Western blot. P38 was used as a loading control

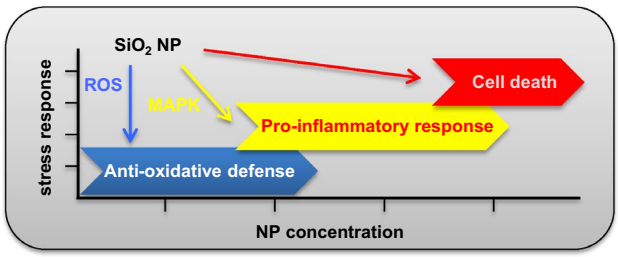

Fig. 8 Revisited hierarchical stress model for silica NPs. Silica NPs trigger a weak anti-oxidative and a clear pro-inflammatory response, whereas at high concentrations cell death ensues. The different tiers of toxicity act independent of each other and different physico-chemical NP properties might be responsible to initiate diverse signalling pathways downstream of separate molecular initiating events. For further details see text

physico-chemical NP properties might be responsible to initiate the separate stress pathways (see also Fig. 8). Therefore, for the implementation of the "safe by design" concept multiple adverse responses need to be considered to tune the relevant material properties accordingly.

Discussion

For the safe development of nanotechnology we need to assess adverse effects of nanomaterials (Gebel et al. 2014; Lynch et al. 2014). Mostly toxicity is monitored by several endpoints without a clear knowledge of the underlying toxicity pathways. Naturally, studies on toxicodynamics are lagging behind as first clear toxicity read outs for a given material need to be defined.

In the case of amorphous silica, we investigated systematically the impact on the three different tiers of toxicity according to the oxidative stress model. Although, in our previous studies we could not detect increased ROS production (Panas et al. 2013), here we demonstrate a mild anti-oxidative response based on gene expression studies. An anti-oxidant inhibited this response, indicating involvement of ROS. Indeed, indirect localized generation of ROS by mitochondria in response to nanosilica exposure has been observed in the past in epithelial cells (Shi et al. 2012) and this might also occur in macrophages. Yet, as the pro-inflammatory response was much more pronounced, we focused on MAPKs as potential mediators to gain more mechanistic insights. Scavenging of ROS did neither interfere with MAPK activation nor reduced cytokine expression in macrophages. Therefore, mediators other than ROS have to be identified which are required for MAPK activation and pro-inflammatory gene expression provoked by nanosilica. In this context it is interesting to note that scavenger receptor A (SR-A) can bind to and mediate uptake of nanosilica, presumably via clathrin-mediated endocytosis, in RAW264.7 cells and in its absence TNF-α secretion is impaired (Orr et al. 2011; Mortimer et al. 2014). SR-A might bind to nanosilica and subsequently induce signaling to MAPKs thereby regulating pro-inflammatory responses. Other receptors such as the mannose receptor (Gallud et al. 2017) or the macrophage receptor with collagenous structure (MARCO) (Hamilton et al. 2006) have also been implicated in the recognition and uptake of micron-sized amorphous and crystalline silica particles, respectively, and might be interesting candidates to initiate MAPK signalling in response to nanosilica. Interestingly, the different MAPK family members specifically regulated different pro-inflammatory targets in response to nanosilica (for a summary see also Fig. S9). Therefore, tissue specific deletion of the various MAPKs in, e.g. macrophages might selectively impair adverse effects of nanosilica, a topic which warrants further investigations.

At high concentrations, nanosilica also triggered cell death in macrophages, which could not be prevented by preincubation with the antioxidant NAC in line with findings

by others (Shi et al. 2012). Microscopic analysis revealed signs of apoptosis (partial chromatin condensation) but also necrosis (increased staining by propidium iodide). Increased membrane damage in response to nanosilica was also evident by enhanced release of LDH. That nanosilica induces apoptosis in RAW264.7 macrophages is supported by previous studies showing increased activity of caspase-3 (Wilhelmi et al. 2012). Whether the parallel increase in membrane leakage as observed by us is due to secondary necrosis of initially apoptotic cells or is a direct effect of nanosilica on membrane integrity of apoptotic cells needs to be addressed in future studies. Signalling events leading to MAPK activation at lower doses can be distinguished from cytotoxic responses at high doses which might act synergistically to even further enhance MAPK signalling. Similar to the situation for most other nanomaterials, the molecular initiating events to promote stress signalling, i.e. in the case of nanosilica to trigger MAPK activation, remains elusive at present. Most likely the pristine silica surface interacts with sensitive biomolecular targets at the cell membrane to perturb membrane integrity but also to initiate signalling events. Indeed, the presence of serum proteins abrogates toxicity (Al-Rawi et al. 2011; Gehrke et al. 2013; Docter et al. 2014) due to the formation of a protein-corona (Neagu et al. 2017) by adsorption to the NP surface (Lesniak et al. 2012; Ruh et al. 2012; Panas et al. 2013; Ge et al. 2015). Therefore, we would like to speculate that in the absence or upon removal of a biomolecular corona the toxicity of silica unfolds. Future studies could try to purify potential receptors, which bind to nanosilica and possibly transduce an apical signal to downstream MAPKs. Alternatively, unbiased RNA interference screening approaches by down regulation of target gene expression seem feasible in transformed macrophages (Sun et al. 2016) and in combination with high throughput immunofluorescence assays to monitor MAPK phosphorylation might be capable to identify upstream regulators. Unravelling the molecular architecture of the signalling pathway culminating in MAPK activation would not only be of relevance to fully understand the mechanism of nanosilica induced inflammation but should also be investigated for its contribution to the toxicity of other nanomaterials.

With respect to the pathophysiological relevance of our findings, induction of TNF-α, MCP-1 and Cxcl2 (MIP2) in macrophages in vivo might be responsible for the enhanced neutrophil recruitment observed after exposure to amorphous nanosilica (Thorley et al. 2007).

Recruitment of neutrophils is one of the hallmarks of nanosilica induced adverse effects in the lung. At present the individual role of the different cell types, especially epithelial cells and macrophages, in the initiation of an inflammatory response still remains unknown. Therefore, it is tempting to speculate that upon nanosilica exposure macrophages act not only as scavengers but also as central early apical inducers of an adaptive response. Specifically the release of TNF-α by macrophages in response to nanosilica is of interest as TNF-α is critical for neutrophil recruitment in the lung early in the inflammatory response triggered by different particles (Driscoll 2000). Recently, in vitro experiments with alveolar macrophages in the absence of serum have been demonstrated to predict the short-term inhalation toxicity in vivo for 18 different nanomaterials including nanosilica (Wiemann et al. 2016). Hence, further mechanistic studies in vitro along with selected confirmatory in vivo experiments on the activation of the MAPK pathway and the subsequent release of the cytokines TNF-α, MCP-1 and Cxcl2 are justified to ultimately explain the pulmonary toxicity of nanosilica.

Conclusion

In conclusion, the hypothesis of a tiered approach to explain (nano)particle toxicity whereby increasing particle concentrations trigger ROS production followed by an enhanced anti-oxidative response to finally boost inflammation culminating in cell death (Nel et al. 2006) may need to be revisited. Future work would need to address the relevance of size, i.e. whether nanoscaled silica behaves really different from microsized silica. To this end, detailed dose–response experiments are necessary as well as various metrics (e.g. specific surface area, mass, particle number) need to be carefully evaluated. Moreover, the chemical composition of various (nano)materials is of obvious importance to assess the general relevance of our findings observed here for nanosilica. As exemplified for nanosilica in our study, the three tiers appear not to be functionally linked. Whereas the anti-oxidative response is dependent on ROS, the pro-inflammatory MAPK pathway operates downstream of other primary targets. Clearly, MAPKs regulate pro-inflammatory gene expression but not cell death and hence both processes are mechanistically different events. Moreover, the MAPKs ERK and JNK seem to selectively control specific pro-inflammatory markers and therefore might contribute to different aspects of inflammation in response to nanosilica (for a summary model see also Fig. 8 and S9).

Acknowledgements CM was funded by the Federal Institute for Risk Assessment (BfR), Germany (BfR-ZEBET-1328-209) which is greatly acknowledged. All other authors were financially supported by the Karlsruhe Institute of Technology.

Compliance with ethical standards

Conflict of interest The authors declare that they have no conflict of interest.

Ethical approval This article does not contain any studies with human participants or animals performed by any of the authors.

References

Al-Rawi M, Diabaté S, Weiss C (2011) Uptake and intracellular localization of submicron and nano-sized SiO(2) particles in HeLa cells. Arch Toxicol 85:813–826

Ambrogio MW, Thomas CR, Zhao YL, Zink JI, Stoddart JF (2011) Mechanized silica nanoparticles: a new frontier in theranostic nanomedicine. ACC Chem Res 44:903–913

Dilger M, Orasche J, Zimmermann R, Paur HR, Diabaté S, Weiss C (2016) Toxicity of wood smoke particles in human A549 lung epithelial cells: the role of PAHs, soot and zinc. Arch Toxicol 90:3029–3044

Docter D, Bantz C, Westmeier D, Galla HJ, Wang Q, Kirkpatrick JC, Nielsen P, Maskos M, Stauber RH (2014) The protein corona protects against size- and dose-dependent toxicity of amorphous silica nanoparticles. Beilstein J Nanotechnol 5:1380–1392

Donauer J, Schreck I, Liebel U, Weiss C (2012) Role and interaction of p53, BAX and the stress-activated protein kinases p38 and JNK in benzo(a)pyrene-diolepoxide induced apoptosis in human colon carcinoma cells. Arch Toxicol 86:329–337

Driscoll KE (2000) TNF alpha and MIP-2: role in particle-induced inflammation and regulation by oxidative stress. Toxicol Lett 112:177–183

Fritsch-Decker S, Both T, Mülhopt S, Paur HR, Weiss C, Diabaté S (2011) Regulation of the arachidonic acid mobilization in macrophages by combustion-derived particles. Part Fibre Toxicol 8:23

Fruijtier-Pölloth C (2016) The safety of nanostructured synthetic amorphous silica (SAS) as a food additive (E 551). Arch Toxicol 90:2885–2916

Gaestel M, Kotlyarov A, Kracht M (2009) Targeting innate immunity protein kinase signalling in inflammation. Nat Rev Drug Discov 8:480–499

Gallud A, Bondarenko O, Feliu N, Kupferschmidt N, Atluri R, Garcia-Bennett A, Fadeel B (2017) Macrophage activation status determines the internalization of mesoporous silica particles of different sizes: exploring the role of different pattern recognition receptors. Biomaterials 121:28–40

Ge C, Tian J, Zhao Y, Chen C, Zhou R, Chai Z (2015) Towards understanding of nanoparticle-protein corona. Arch Toxicol 89:519–539

Gebel T, Foth H, Damm G, Freyberger A, Kramer PJ, Lilienblum W, Röhl C, Schupp T, Weiss C, Wollin KM, Hengstler JG (2014) Manufactured nanomaterials: categorization and approaches to hazard assessment. Arch Toxicol 88:2191–2211

Gehrke H, Frühmesser A, Pelka J, Esselen M, Hecht LL, Blank H, Schuchmann HP, Gerthsen D, Marquardt C, Diabaté S, Weiss C, Marko D (2013) In vitro toxicity of amorphous silica nanoparticles in human colon carcinoma cells. Nanotoxicology 7:274–293

Haase A, Dommershausen N, Schulz M, Landsiedel R, Reichardt P, Krause BC, Tentschert J, Luch A (2017) Genotoxicity testing of different surface-functionalized SiO_2, ZrO_2 and silver nanomaterials in 3D human bronchial models. Arch Toxicol 91:3991–4007

Hamilton RF Jr, Thakur SA, Mayfair JK, Holian A (2006) MARCO mediates silica uptake and toxicity in alveolar macrophages from C57BL/6 mice. J Biol Chem 281:34218–34226

Hansjosten I, Rapp J, Reiner L, Vatter R, Fritsch-Decker S, Peravali R, Palosaari T, Joossens E, Gerloff K, Macko P, Whelan M, Gilliland D, Ojea-Jimenez I, Monopoli MP, Rocks L, Garry D, Dawson K, Röttgermann PJF, Murschhauser A, Rädler JO, Tang SVY, Gooden P, Belinga-Desaunay MA, Khan AO, Briffa S, Guggenheim E, Papadiamantis A, Lynch I, Valsami-Jones E, Diabaté S, Weiss C (2018) Microscopy-based high-throughput assays enable multi-parametric analysis to assess adverse effects of nanomaterials in various cell lines. Arch Toxicol 92:633–649

Herrlich P, Karin M, Weiss C (2008) Supreme EnLIGHTenment: damage recognition and signaling in the mammalian UV response. Mol Cell 29:279–290

Lee S, Yun HS, Kim SH (2011) The comparative effects of mesoporous silica nanoparticles and colloidal silica on inflammation and apoptosis. Biomaterials 32:9434–9443

Lesniak A, Fenaroli F, Monopoli MP, Aberg C, Dawson KA, Salvati A (2012) Effects of the presence or absence of a protein corona on silica nanoparticle uptake and impact on cells. ACS Nano 6:5845–5857

Lynch I, Weiss C, Valsami-Jones E (2014) A strategy for grouping of nanomaterials based on key physico-chemical descriptors as a basis for safer-by-design NMs. Nano Today 9:266–270

Marquardt C, Fritsch-Decker S, Al-Rawi M, Diabaté S, Weiss C (2017) Autophagy induced by silica nanoparticles protects RAW264.7 macrophages from cell death. Toxicology 379:40–47

Maser E, Schulz M, Sauer UG, Wiemann M, Ma-Hock L, Wohlleben W, Hartwig A, Landsiedel R (2015) In vitro and in vivo genotoxicity investigations of differently sized amorphous SiO_2 nanomaterials. Mutat Res Genet Toxicol Environ Mutagen 794:57–74

Moret F, Selvestrel F, Lubian E, Mognato M, Celotti L, Mancin F, Reddi E (2015) PEGylation of ORMOSIL nanoparticles differently modulates the in vitro toxicity toward human lung cells. Arch Toxicol 89:607–620

Morishige T, Yoshioka Y, Inakura H, Tanabe A, Narimatsu S, Yao X, Monobe Y, Imazawa T, Tsunoda S, Tsutsumi Y, Mukai Y, Okada N, Nakagawa S (2012) Suppression of nanosilica particle-induced inflammation by surface modification of the particles. Arch Toxicol 86:1297–1307

Mortimer GM, Butcher NJ, Musumeci AW, Deng ZJ, Martin DJ, Minchin RF (2014) Cryptic epitopes of albumin determine mononuclear phagocyte system clearance of nanomaterials. ACS Nano 8:3357–3366

Murugadoss S, Lison D, Godderis L, van den Brule S, Mast J, Brassinne F, Sebaihi N, Hoet PH (2017) Toxicology of silica nanoparticles: an update. Arch Toxicol 91:2967–3010

Neagu M, Piperigkou Z, Karamanou K, Engin AB, Docea AO, Constantin C, Negrei C, Nikitovic D, Tsatsakis A (2017) Protein biocorona: critical issue in immune nanotoxicology. Arch Toxicol 91:1031–1048

Nel A, Xia T, Mädler L, Li N (2006) Toxic potential of materials at the nanolevel. Science 311:622–627

Nyström AM, Fadeel B (2012) Safety assessment of nanomaterials: implications for nanomedicine. J Control Release 161:403–408

Orr GA, Chrisler WB, Cassens KJ, Tan R, Tarasevich BJ, Markillie LM, Zangar RC, Thrall BD (2011) Cellular recognition and trafficking of amorphous silica nanoparticles by macrophage scavenger receptor A. Nanotoxicology 5:296–311

Panas A, Marquardt C, Nalcaci O, Bockhorn H, Baumann W, Paur HR, Mülhopt S, Diabaté S, Weiss C (2013) Screening of different metal oxide nanoparticles reveals selective toxicity and inflammatory potential of silica nanoparticles in lung epithelial cells and macrophages. Nanotoxicology 7:259–273

Robinson MA, Baumgardner JE, Otto CM (2011) Oxygen-dependent regulation of nitric oxide production by inducible nitric oxide synthase. Free Radic Biol Med 51:1952–1965

Ruh H, Kühl B, Brenner-Weiss G, Hopf C, Diabaté S, Weiss C (2012) Identification of serum proteins bound to industrial nanomaterials. Toxicol Lett 208:41–50

Schreck I, Chudziak D, Schneider S, Seidel A, Platt KL, Oesch F, Weiss C (2009) Influence of aryl hydrocarbon-(Ah) receptor and genotoxins on DNA repair gene expression and cell survival of mouse hepatoma cells. Toxicology 259:91–96

Shi J, Karlsson HL, Johansson K, Gogvadze V, Xiao L, Li J, Burks T, Garcia-Bennett A, Uheida A, Muhammed M, Mathur S, Morgenstern R, Kagan VE, Fadeel B (2012) Microsomal glutathione transferase 1 protects against toxicity induced by silica nanoparticles but not by zinc oxide nanoparticles. ACS Nano 6:1925–1938

Sun J, Li N, Oh KS, Dutta B, Vayttaden SJ, Lin B, Ebert TS, De ND, Davis J, Bagirzadeh R, Lounsbury NW, Pasare C, Latz E, Hornung V, Fraser ID (2016) Comprehensive RNAi-based screening of human and mouse TLR pathways identifies species-specific preferences in signaling protein use. Sci Signal 9:ra3

Tang L, Fan TM, Borst LB, Cheng J (2012) Synthesis and biological response of size-specific, monodisperse drug-silica nanoconjugates. ACS Nano 6:3954–3966

Thorley AJ, Ford PA, Giembycz MA, Goldstraw P, Young A, Tetley TD (2007) Differential regulation of cytokine release and leukocyte migration by lipopolysaccharide-stimulated primary human lung alveolar type II epithelial cells and macrophages. J Immunol 178:463–473

Wagner EF, Nebreda AR (2009) Signal integration by JNK and p38 MAPK pathways in cancer development. Nat Rev Cancer 9:537–549

Wiemann M, Vennemann A, Sauer UG, Wiench K, Ma-Hock L, Landsiedel R (2016) An in vitro alveolar macrophage assay for predicting the short-term inhalation toxicity of nanomaterials. J Nanobiotechnol 14:16

Wilhelmi V, Fischer U van, Schulze-Osthoff BD, Schins K, Albrecht RP, C (2012) Evaluation of apoptosis induced by nanoparticles and fine particles in RAW 264.7 macrophages: facts and artefacts. Toxicol In Vitro 26:323–334

Zitvogel L, Kepp O, Kroemer G (2010) Decoding cell death signals in inflammation and immunity. Cell 140:798–804